J Geod (2014) 88:601–615
DOI 10.1007/s00190-014-0709-9

ORIGINAL ARTICLE

Realization of a consistent set of vertical reference surfaces in coastal areas

D. C. Slobbe · R. Klees · B. C. Gunter

Received: 10 July 2013 / Accepted: 25 February 2014 / Published online: 26 March 2014

Abstract We present a combined approach for the realization of the (quasi-)geoid as a height reference surface and the vertical reference surface at sea (chart datum). This approach, specifically designed for shallow seas and coastal waters, provides the relation between the two vertical reference surfaces without gaps down to the coast. It uses a regional hydrodynamic model, which, after vertical referencing, provides water levels relative to a given (quasi-)geoid. Conversely, the hydrodynamic model is also used to realize a (quasi-)geoid by providing corrections to the dynamic sea surface topography, which are used to reduce radar altimeter-derived sea surface heights to the (quasi-)geoid. The coupled problem of vertically referencing the hydrodynamic model and computing the (quasi-)geoid is solved iteratively. After convergence of the iteration process, the vertically referenced hydrodynamic model is used to realize the chart datum. In this way, consistency between the chart datum and (quasi-) geoid is ensured. We demonstrate the feasibility and performance of this approach for the Dutch mainland and North Sea. We show that in the Dutch part of the North Sea, the differences between modeled and observed instantaneous and mean dynamic sea surface topography is 8–10 and 5.8 cm, respectively. On land, we show that the methodology provides a quasi-geoid which has a lower standard deviation (SD) than the European Gravimetric Geoid 2008 (EGG08) and the official Netherlands quasi-geoid NLGEO2004-grav when compared to GPS-levelling data. The root mean square at 81 GPS-levelling points is below 1.4 cm; no correction surface is needed. Finally, we show that the chart datum (lowest astronomical tide, LAT) agrees with the observed chart datum at 92 onshore tide gauges to within 21.5 cm (SD).

Keywords Vertical reference surfaces · Quasi-geoid · Lowest astronomical tide · Hydrodynamic model

1 Introduction

Many coastal countries lack an accurate and continuous model of the relation between the onshore and offshore vertical reference surfaces (VRSs). Usually, this relation is properly established only at the onshore tide gauges. For many applications, this is not sufficient. An example is coastal zone management, which requires that land/sea datasets be processed in the same coordinate system. Accuracy requirements may be quite high, e.g., one decimeter in the southern North Sea and along the shipping routes to the harbors of Antwerp and Rotterdam. Here, we suggest a methodology which provides an accurate and continuous model of the relation between the onshore and offshore VRSs over the whole domain of the offshore VRS, including the coastal waters. We demonstrate the feasibility and performance of the suggested methodology for the Dutch North Sea and coastal waters using real data.

A geoid, or quasi-geoid, is commonly used as an onshore VRS ["height reference surface (HRS)"]. Offshore, various tidal datums are used ["chart datum (CD)"]. The most important CD is the LAT, which is defined as "the lowest tide level that can be predicted to occur under average meteorological conditions and under any combination of astronomical conditions" (International Hydrographic Organization 1994). The International Hydrographic Organization (IHO) adopted the

D. C. Slobbe (✉) · R. Klees · B. C. Gunter
Delft University of Technology, P.O. Box 5048,
2600 GA Delft, The Netherlands
e-mail: D.C.Slobbe@tudelft.nl

B. C. Gunter
Daniel Guggenheim School of Aerospace Engineering,
Georgia Institute of Technology, Atlanta, GA 30332-0150, USA

LAT as CD (International Hydrographic Organization 2011), at least for areas where the tides have an appreciable effect on the water level. In the remaining part of the paper, we assume that the (quasi-)geoid is adopted as the HRS and the LAT as the CD. The methodology to be presented, however, is also applicable if another tidal surface is used as CD. At sea, we frequently do not distinguish between geoid and quasi-geoid and use both names simultaneously. This is justified because the differences between the two VRSs are negligible given the target accuracy.

The relation between HRS and CD is established as soon as both are realized relative to the same reference ellipsoid in a well-defined terrestrial reference system. Contrary to the HRS, a 3D description of the CD that includes the coastal waters [referred to here as a coastal-waters-inclusive continuous (CWIC) model] cannot be derived purely from observations. This requires time series of the instantaneous water level relative to a reference ellipsoid collected over a sufficiently long period of time and at a sufficiently spatially dense set of points. The time series should also have sufficient temporal resolution to resolve all relevant tidal constituents that are needed to reconstruct the tidal water levels from which CD is derived. From the existing measurement techniques that provide time series of instantaneous water levels, radar altimetry, tide gauges, and GNSS buoys, it are the altimetry products that provide a time series over a sufficiently long period and, in open sea, with sufficient spatial resolution. Radar altimetry, however, lacks the required temporal resolution. Tide gauges and GNSS buoys, on the other hand, provide time series that are sufficiently long and do have sufficient temporal resolution, but their spatial coverage is poor.

Therefore, the current practice to obtain a CWIC model of the ellipsoidal heights of CD in shallow seas and coastal waters is to determine them as the difference between the ellipsoidal heights of the mean sea level (MSL) and the separation between CD and MSL. The former is derived from radar altimeter data; the latter is taken from a global or regional ocean tide model. At tide gauges, ellipsoidal heights of CD are determined from Global Navigation Satellite System (GNSS) ellipsoidal heights and the observed water levels. This approach is, for instance, applied in the US VDatum project (Parker et al. 2003; Myers et al. 2005) and in the UK Vertical Offshore Reference Frame (VORF) project (Ziebart et al. 2007). The major problem of this approach, however, is that no accurate continuous relation of the HRS and the CD is obtained in coastal waters. The reason is that due to the reduced accuracy of radar altimeter data in coastal regions (e.g., Andersen and Knudsen 2000; Deng et al. 2002), coastal waters lack information about the MSL. Even when using the most advanced retracking schemes (Deng 2003; Gommenginger et al. 2011), the data gap along the coastline will still be several kilometers (Gommenginger et al. 2011). An expensive and, hence, non-preferable solution is to close the gap by GNSS surveys (e.g., Pineau-Guillou and Dorst 2011). Closing it using MSL values derived from tide gauge records (Iliffe et al. 2007) requires spatial interpolation. This interpolation is not trivial as the sea-level behavior at a particular tide gauge location close to the coast, and hence, the MSL may be strongly anisotropic. Furthermore, the distance between neighboring tide gauge locations may be tens of kilometers.

In this paper, we present a solution that omits the use of the MSL as an "intermediate" reference surface and uses instead the only other "observable" reference surface available, which is the (quasi-)geoid. Contrary to the MSL, a high-resolution (quasi-)geoid model in coastal waters can be derived from observations.

Using the (quasi-)geoid as an "intermediate" reference surface, the accuracy of the realization of the CD becomes dependent on the accuracy of the used (quasi-)geoid model. Indeed, errors in the (quasi-)geoid map one-to-one to the ellipsoidal heights of the CD. Therefore, aiming for the highest possible (quasi-)geoid accuracy is a must in obtaining a CWIC realization of the CD. Obviously, the quality of the (quasi-)geoid strongly depends on the availability and quality of data. The fact that, so far, in the computation of most available (quasi-)geoid models, no GOCE data have been used (indeed, these data became publicly available since May 2010 and also the data processing is still being improved) already suggests that there is space for improvements. This suggestion is supported by the assessment conducted by Farahani et al. (2013a), who quantified the added value of GOCE data to be 25–38 % in the continental areas poorly covered with terrestrial gravimetry data (Equatorial Africa, Himalayas, and South America), 7–17 % in those with a good coverage with these data (Australia, North America, and North Eurasia), and 14 % in the oceans.

However, especially for the coastal countries (with shallow offshore waters), there is another aspect to be taken into account when aiming at a highly accurate (quasi-)geoid. Offshore, the available data are usually limited to radar altimeter data. Locally, they are supplemented with shipboard and/or airborne gravity data. The use of radar altimeter data requires, among others, a correction of the observed sea surface heights (SSHs) or SSH slopes for the contribution of the dynamic sea surface topography. The latter consists of three components: ocean tides, wind- and pressure-driven (surge), and density-driven (baroclinic) water level variations, of which the first is often the largest. Usually, the ocean tide corrections are obtained from a global ocean tide model. Several authors (e.g., Andersen and Knudsen 2000; Hwang et al. 2006; Sandwell and Smith 2009) have suggested that corrections obtained from such *global* models lack accuracy in shallow waters and recommended the use of specifically designed regional tide models. The same applies to the inverted barometer correction that is, if not ignored altogether, often used as an approximation to the surge component (e.g., Hwang et al. 2006). This correction lacks accuracy because when used in shallow waters, it ignores the dominant acceleration term related to wind stress. In addition, away from the boundary currents, the baroclinic component is often ignored or only the time-averaged contribution is removed. In this study, the individual contributors to the dynamic sea surface topography are treated as one integral phenomenon that will be derived from a regional hydrodynamic model. In Slobbe and Klees (2014), we show the better performance of these corrections compared to tidal corrections derived from the global ocean tide model GOT4.7 (Ray 1999), surge corrections derived from the MOG2D model (Carrère and Lyard 2003), and corrections for the time-averaged baroclinic contribution computed as differences between the DTU10 mean sea surface model (Andersen 2010), and the EGG08 quasi-geoid (Denker 2013).

Traditionally, (quasi-)geoid realization and CD realization are considered as two separate tasks belonging to different disciplines: geodesy and hydrography. However, there are at least two reasons why it may be beneficial to combine the realization of both VRSs. First, the (quasi-)geoid is needed to realize a CD model that includes the coastal waters. Second, the same "tool" (a regional hydrodynamic model) required to realize the CD helps to improve the (quasi-)geoid. The latter also ensures consistency between both VRSs. In this paper, we present such a *combined* approach.

The work presented here builds on our work presented in Slobbe et al. (2013a); Slobbe et al. (2013b) and Slobbe and Klees (2014). The latter paper (Slobbe and Klees 2014) examines the impact of sea surface dynamic topography (DT) corrections to be applied to altimeter-derived sea surface slopes on the quasi-geoid in the shallow and coastal waters of the North Sea. In Slobbe et al. (2013a), we presented and evaluated several strategies to obtain a regional hydrodynamic model that provides water levels relative to a (quasi-)geoid. Slobbe et al. (2013b) presents two realizations of LAT relative to the EGG08 quasi-geoid and presents the validation results of one of these. In this paper, we present a combined approach for the realization of both the (quasi-)geoid and LAT, and we present and validate a new quasi-geoid model for the Dutch waters and mainland, called NLGEO2013. Furthermore, we summarize the results of one experiment presented and discussed in (Slobbe et al. 2013a) that we repeated in this study over a much longer time span (20 years instead of 3 years). Finally, we present and validate the LAT realization adopted by the Hydrographic Service of the Royal Netherlands Navy.

The paper is organized as follows: in Sect. 2, we describe the methodology. In Sect. 3, we demonstrate the feasibility and performance of the methodology in a test area using real data. In particular, we provide some information about the regional hydrodynamic model used in this study and all datasets used to compute (i) the sea surface DT corrections to the altimeter SSHs, (ii) the quasi-geoid, and (iii) the LAT relative to this quasi-geoid. In Sect. 4, we assess the ability of the regional hydrodynamic model to represent the time-averaged and instantaneous water levels, and present and validate the computed VRSs. Section 5 contains a summary and the main conclusions.

2 Methodology

In this section, we present the methodology to compute consistent realizations of the onshore and offshore VRSs that have a precisely defined relationship everywhere, including the coastal waters. Without loss of generality, we assume that LAT is the CD; adaptation to any other tidal datum is straightforward. First, we present two alternative approaches to use the (quasi-)geoid in a CD realization and we justify our choice for one of them. Thereafter, we discuss the key problem of the pursued methodology, i.e., to ensure that the water levels of a regional hydrodynamic model refer to a given (quasi-)geoid. We present and discuss two solutions to this problem. They differ from each other in the extent and way the (quasi-)geoid information is used.

2.1 Realizing LAT relative with respect to a (quasi-)geoid

A CWIC 3D description of LAT can be derived in two different ways, which are illustrated in Fig. 1. Both approaches differ from each other by the reference surface used as the intermediate surface to which the model-derived LAT values refer and, related to that, in the way the average meteorological conditions under which the LAT events are supposed to occur are accounted for (International Hydrographic Organization 2011, Technical Resolution 3/1919).

2.1.1 First approach: via MSL

The first approach (Fig. 1a) determines the ellipsoidal heights of LAT as the sum of the ellipsoidal heights of MSL and the heights of LAT relative to MSL. As such, it is similar to the approach applied in, e.g., the US VDatum project and in the UK VORF project (Sect. 1). The difference is, however, that here the ellipsoidal heights of MSL (h_{MSL}) are derived as the sum of (quasi-)geoid heights (N) and hydrodynamic model-derived MSL expressed relative to that (quasi-)geoid (H_{MSL}) rather than from radar altimeter data. LAT relative to MSL ($\Delta h_{\mathrm{LAT}}^{\mathrm{MSL}}$) is derived from modeled tidal water levels. So,

$$h_{\mathrm{LAT}} = h_{\mathrm{MSL}} + \Delta h_{\mathrm{LAT}}^{\mathrm{MSL}} = N + H_{\mathrm{MSL}} + \Delta h_{\mathrm{LAT}}^{\mathrm{MSL}}. \qquad (1)$$

This approach has two major drawbacks. First of all, an error is introduced when not taking into account that the model's reference surface is an equipotential surface of Earth's gravity field (Hughes and Bingham 2008). The reason is that in shallow seas and coastal waters tides contribute

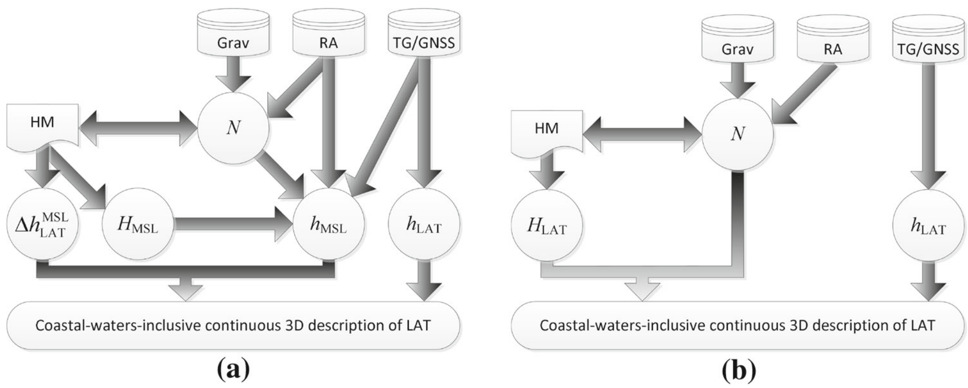

Fig. 1 Schematic representations of two alternative approaches to derive a coastal-waters-inclusive continuous 3D description of LAT. In the first alternative **a** the MSL is used as an intermediate surface, while in the second alternative **b** the (quasi-)geoid is used. In the schemes, we use $\Delta h^{\mathrm{MSL}}_{\mathrm{LAT}}$ for the model-derived separation between the MSL and LAT, H_{MSL} for the model-derived height of the MSL above the (quasi-)geoid, N for the (quasi-)geoid heights, h_{MSL}, h_{LAT} for the ellipsoidal heights of MSL and LAT, respectively, and H_{LAT} for the model-derived separation between the (quasi-)geoid and LAT. The abbreviations HM, Grav, RA, and TG, stand for hydrodynamic model, gravimetry, radar altimetry, and tide gauges, respectively

to the MSL. For instance, Prandle (1978) has shown that the contribution of the M_2 tide to MSL in the southern North Sea varies from -1 to 8 cm, with maximum values along the Dutch coast. Second, as the hydrodynamic model used to derive the separation between MSL and LAT is forced by ocean tides only, it assumes that tide and average meteorological and baroclinic conditions are linearly additive. That is, there are no nonlinear interactions between tide, surge, and baroclinic effects. In shallow seas and coastal waters, this is definitely not the case, at least not for tide and surge, as has been shown by, e.g., Prandle and Wolf (1978), Wolf (1981), and Horsburgh and Wilson (2007).

2.1.2 Second approach: via the (quasi-)geoid

In the second approach (Fig. 1b), the ellipsoidal heights of LAT are computed as the sum of the (quasi-)geoid heights and the heights of LAT relative to the (quasi-)geoid (H_{LAT}):

$$h_{\mathrm{LAT}} = N + H_{\mathrm{LAT}}. \tag{2}$$

The latter can be derived from modeled water levels, which comprise the tide and the time-averaged meteorological and baroclinic contributions, provided that the modeled water levels refer to the (quasi-)geoid. Compared to the first approach, the second one has at least three advantages:

1. It is conceptually clearer since the hydrodynamic model's reference surface, as well as the geoid, is an equipotential surface of the Earth's gravity field (Hughes and Bingham 2008).
2. It accounts for any nonlinear interaction between tide and time-averaged surge.
3. It allows the inclusion of the dominant time variations (i.e., seasonal) in MSL caused by wind, air pressure, and water density when realizing LAT.

Whether nonlinear interactions between tide and surge are relevant depends on their magnitude relative to the target accuracy for the realization of LAT. For instance, Slobbe et al. (2013b) have shown that on the Dutch North Sea, the magnitude of the tide and time-averaged surge interaction is just a few cm. Advantage 3 follows from a more precise interpretation of the LAT definition as the lowest water level to occur under *average meteorological conditions* and under any combination of astronomical conditions. Indeed, since the average meteorological conditions in, e.g., the spring, differ from those in the fall, it makes sense to include the average seasonal variations into the definition of the LAT. This advantage may become significant for safe navigation in very shallow waters, e.g., along the shipping routes in the southern North Sea to the ports of Antwerp and Rotterdam.

To obtain the highest accuracy of the LAT surface, LAT values at onshore and offshore tide gauges need to be integrated in the model-derived LAT surface (cf. Turner et al. 2010). This can be achieved in several ways. Turner et al. (2010) merged LAT values derived from observed water levels and hydrodynamic models in a post-processing step using spatial interpolation. Alternatively, one might consider an online assimilation of tidal water levels into the model. In this study, we rely on the model calibration that has been carried out using both tide gauge and radar altimeter data.

2.2 Vertical referencing of a hydrodynamic model to a particular (quasi-)geoid

Regardless of which of the two approaches outlined in Sect. 2.1 is used, a method needs to be developed which ensures that the water levels of the hydrodynamic model refer to a particular (quasi-)geoid. We call this "vertical referencing" of the hydrodynamic model. In Fig. 1a, b, this is

Table 1 Summary of the approaches to obtain a hydrodynamic model that provides water levels relative to a particular (quasi-)geoid

Approach	Realized by	Source baroclinic contribution	Availability (quasi-)geoid	Iterations
I.1	Properly referenced open boundary conditions + assimilation properly referenced water levels	Radar altimeter data	Hydr. model domain	y
I.2	Idem I.1	Ocean circulation model	Idem I.1	Idem I.1
II.1	Properly referenced open boundary conditions	Radar altimeter data	Open sea boundaries of the hydr. model	y
II.2	Idem II.1	Ocean circulation model	Hydr. model domain	n[a]

[a] Provided the conditions mentioned in the text are met

indicated by the arrow pointing from the (quasi-)geoid to the hydrodynamic model.

However, as discussed in Sect. 1, many coastal countries lack a sufficiently accurate (quasi-)geoid model. Here, two major improvements are (i) the inclusion of GOCE data, and (ii) the use of better radar altimeter data by improving the accuracy of sea surface dynamic topography corrections. The latter should be obtained from a proper regional hydrodynamic model.

Consistency between both the (quasi-)geoid and LAT is guaranteed when, in the realization of both reference surfaces, the same regional hydrodynamic model and the same forcing fields (tides, winds, mean sea-level pressure, temperature and salinity) are used. Therefore, in our approach, the hydrodynamic model used to derive the separation between the (quasi-)geoid and LAT will also be used when computing dynamic topography corrections for the reduction in altimeter-derived SSHs or SSH slopes to the (quasi-)geoid. This actually presents a dilemma; on the one hand, we need to use a hydrodynamic model to derive a proper (quasi-)geoid involving radar altimeter data, while on the other hand, the (quasi-)geoid needs to be the model's reference surface. The solution to this problem depends on how the hydrodynamic model is vertically referenced, which in turn depends on the extent and way the (quasi-)geoid information is used.

Two approaches, briefly summarized in Table 1, are possible. In the remainder of this section, they will be briefly discussed and we justify our choice for one of them.

2.2.1 First approach: open boundary conditions and data assimilation

In the first and most ideal approach, the vertical referencing is realized by (i) referring the water levels along the open sea boundaries to the (quasi-)geoid and (ii) assimilating instantaneous water levels relative to this (quasi-)geoid into the hydrodynamic model. The latter source of information is available at onshore and offshore tide gauges, but also along the ground tracks of radar altimeter satellites. The baroclinic contribution to the instantaneous water levels prescribed at the open sea boundaries is obtained from (i) radar altimeter data or (ii) an ocean circulation model. With this approach, a (quasi-)geoid is needed that covers the whole domain of the used regional hydrodynamic model. If no proper (quasi-)geoid model is available, and if radar altimeter data are needed to compute a sufficiently accurate (quasi-)geoid, an iterative procedure is required to realize both the (quasi-)geoid and the vertical referencing of the model. Starting with an initial (quasi-)geoid model (e.g., EGM2008 Pavlis et al. 2012 or any continental (quasi-)geoid like the EGG08), the hydrodynamic model is vertically referenced to this initial (quasi-)geoid. Thereafter, the modeled water levels relative to the initial (quasi-)geoid are used to correct altimeter-derived SSHs or SSH slopes for the sea surface dynamic topography before they are used to compute an improved (quasi-)geoid. In the next iteration, the improved (quasi-)geoid is used as the initial one and the procedure is iterated until differences between two successive (quasi-)geoids are below some user-specified threshold.

2.2.2 Second approach: open boundary conditions only

In the second approach, the assimilation of instantaneous water levels is omitted. Again, the baroclinic contribution to the instantaneous water levels prescribed at the open sea boundaries is obtained from (i) radar altimeter data or (ii) an ocean circulation model. Both variants have been investigated in Slobbe et al. (2013a). If variant (i) is followed, the (quasi-)geoid is only needed along the open sea boundaries, and the same iterative approach as described before can be implemented if no proper (quasi-)geoid model is available and if radar altimeter data are needed to compute a sufficiently accurate (quasi-)geoid. If variant (ii) is followed, the domain of the ocean circulation model must comprise the domain of the regional hydrodynamic model. In addition, the (quasi-)geoid is needed over the domain of the ocean circulation model to estimate the datum shift between the reference surface of the ocean circulation model and the (quasi-)geoid. In Slobbe et al. (2013a), we computed the latter as the spatially integrated, smoothed difference between an observation-derived MDT and the MDT computed with the ocean circulation model, where regions prone to errors both in the observation- and model-derived MDT's (coastal regions and regions along the open boundaries of the used ocean circulation model) are excluded. If a new (quasi-) geoid model needs to be computed using among others radar altimeter data, no iterative approach is needed, provided that at least one of the following conditions is met:

1. radar altimeter data are used in the form of deflections of the vertical (DoVs) or differenced heights (Hwang and Hsu 2008);
2. we adopt the datum choice of our initial (quasi-)geoid and the quality of the initial (quasi-)geoid is reasonable.

In the latter case, we can safely assume that differences in the datum shift computed using an observation-derived MDT relative to the initial (quasi-)geoid and one relative to the computed (quasi-)geoid are negligible.

2.2.3 Our choice

In this study, we prefer the second approach, variant (ii). The assimilation of instantaneous water levels in the model domain helps to prevent a leakage of errors in the modeled water levels into the (quasi-)geoid realization. This assimilation, however, is not always possible as it requires a substantial numerical effort. Moreover, the temporal sampling may not be enough to have a significant effect on the output water levels. The choice for variant (ii) is based on the results of a study presented in Slobbe et al. (2013a). In this study, it was shown that deriving the baroclinic component to the prescribed water levels from radar altimeter data does not result in an improved representation of the instantaneous water levels. Hence, this variant does not provide much advantage compared to obtaining the baroclinic component from modeled water levels. Obtaining it from modeled water levels is much easier to implement and makes, subject to the conditions specified above, iterations superfluous.

3 Application

In the second part of the paper, we demonstrate the applicability and performance of the chosen methodology using real data. The test area is the Dutch mainland and North Sea (cf. Fig. 2).

3.1 The hydrodynamic model and forcing data

The numerical model used in this study is the *extended* Dutch Continental Shelf Model (DCSM) version 5 described by Slobbe et al. (2013a), with the original DCSM model is described by Gerritsen et al. (1995) and Verlaan et al. (2005). The model is based on the WAQUA software package

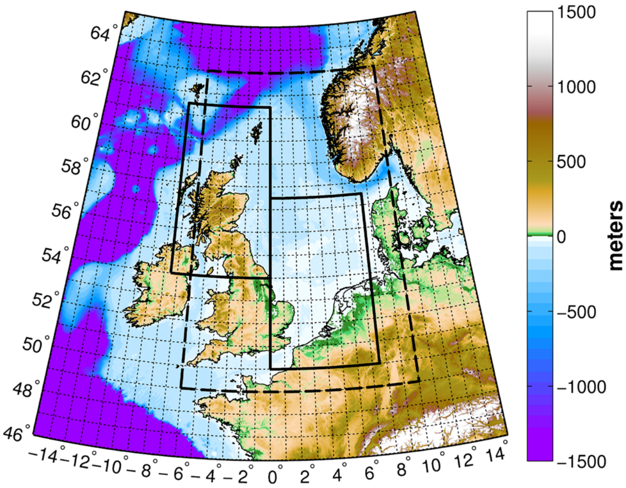

Fig. 2 Outline of the two subregions used to obtain proper values for the bandwidth and number of SRBFs on top of the GEBCO_08 grid (General Bathymetric Chart of the Oceans (GEBCO) 2012). The subregion indicated by the dashed line is the domain used to estimate the variance components by MCVCE. The region shown in this *map* is the whole computational domain of NLGEO2013

(Leendertse 1967; Stelling 1984) for depth-integrated flow. WAQUA includes the nonlinear surge–tide interaction and is based on the depth-integrated shallow water equations.

The DCSM covers the area of the northwest European continental shelf to at least the 200 m depth contour, i.e., 12°W–13°E and 48°N–62.3°N, and has a horizontal resolution of $1/8° \times 1/12°$ (approximately 8×9 km) in east–west and north–south directions, respectively. The model was extended to account for depth-averaged water density variations as described in Slobbe et al. (2013a). To obtain a unique solution of the depth-integrated shallow water equations, a set of boundary conditions is prescribed. At the *open* sea boundaries, water levels are prescribed as discussed in detail in Slobbe et al. (2013a).

Wind and air pressure data are obtained from the publicly available data of the interim reanalysis project, ERA-Interim (Dee et al. 2011), provided by the European Center for Medium-Range Weather Forecasts (ECMWF). ERA-Interim covers the period from January 1, 1979, onwards and provides three-hourly grids with a spatial resolution of $1.5° \times 1.5°$ (recently this has been increased to $0.75° \times 0.75°$).

Salinity and temperature fields used in the computation of the depth-averaged baroclinic pressure gradients are obtained from the Atlantic—European North West Shelf—Ocean Physics Hindcast provided by the Proudman Oceanographic Laboratory (POL), hereafter referred to as POL's hindcast (Holt et al. 2005). This hindcast over 45 years (1960–2004) was carried out with the Atlantic Margin Model, a coupled hydrodynamic-ecosystem model. The hydrodynamics are provided by the POL 3D baroclinic model (POL3DB) (Holt and James 2001; Holt et al. 2001). The output, provided as monthly mean fields, includes the sea surface height, potential temperature, and salinity of the sea water.

3.2 The data needed to compute the quasi-geoid

3.2.1 Gravity data

The *reference field* used in the remove-compute-restore (RCR) procedure is the Delft Gravity Model (DGM-1S) (Farahani et al. 2013a,b). DGM-1S is a GRACE/GOCE-combined gravity field model complete to degree 250.

The *terrestrial pointwise free-air gravity anomaly* (FAA) datasets include those used to compute the Dutch quasi-geoids NLGEO2004 (Crombaghs and de Bruijne 2004) and NLGEO2007 (Klees et al. 2008). These were complemented by pointwise FAAs in Belgium, Denmark, France, and Germany obtained from the Bureau Gravimétrique International, Bundesamt für Kartographie und Geodäsie, and the Nordic Geodetic Commission, respectively. The total set comprises 148,004 terrestrial measurements. The dataset is complemented by *DoVs in the north–south and east–west directions from EGG08* in Norway and the UK. No terrain corrections have been applied to the FAAs in the mountainous areas, as we expect that this has a negligible influence on the computed quasi-geoid over the Dutch mainland and North Sea.

Shipboard FAAs are obtained from different global and regional databases. These data include, among others, the data acquired by Rijkswaterstaat (the Dutch Department of Public Works) and Shell in the Dutch IJssel Lake and Wadden Sea, respectively, that have been used in the computation of NLGEO2004 and NLGEO2007. Also the data acquired by Delft University of Technology in 1986 during the "Navigation and Gravimetric Experiment" at the North Sea (Haagmans et al. 1988) are included and a dataset obtained from the British Geological Service (BGS). Part of the systematic errors in the shipboard gravity data is removed by adding for each survey the average difference between the observed and altimeter-derived FAAs obtained from the DTU10 global (on land EGM2008 is used) gravity field model (Andersen et al. 2010; Andersen 2010). After removing the systematic errors, we used the pointwise differences between the shipboard and DTU10-GRA FAAs to remove outliers in the data set. The outliers are identified using subsequently the 10-sigma and 3-sigma rules, i.e., observations are identified as outliers if the differences between the shipboard and DTU10-GRA FAAs are larger than ten/three times the SD of all differences. Here, we first apply the 10-sigma rule to avoid a contamination of the SD by extremely large outliers. In total, 568,167 shipboard measurements are used.

Finally, we use the *airborne gravity disturbances* acquired from 2006–2008 during the BalGRACE and NorthGRACE campaigns (Schäfer et al. 2008) and the data acquired as part of the "airborne geoid mapping system for coastal oceanography" project (Forsberg et al. 1997). This observation group comprises 8,360 measurements.

3.2.2 Along-track DoVs from radar altimeter data

Radar altimeter data are used in the form of along-track DoVs. In this way, long-wavelength errors (e.g., radial orbit errors) are suppressed and many of the corrections needed to recover the temporal variations in ocean surface height associated with currents, and eddies become largely unimportant for the recovery of the gravity field because the slope of these corrections is far less than the slope error in the radar altitude measurement (e.g., Sandwell and Smith 2009).

The data are obtained from two sources. 1 Hz radar data acquired by the ERS-1 (exact repeat mission (ERM) + geodetic mission (GM) phases), ERS-2, Envisat, GEOSAT (GM phase), GFO-1, Jason-1/2, and TOPEX/POSEIDON (T/P) satellites during the period March 1985–September 2011 are extracted from the Radar Altimeter Database System (RADS) (Scharroo 2013). For a part of our computational domain (comprising the whole North Sea), the ERS-1 GM data are replaced by retracked data kindly provided by P. A. M. Berry from the Earth and Planetary Remote Sensing (EAPRS) Laboratory of the De Montford University. These retracked 20-Hz data represent the uncorrected ellipsoidal heights of the instantaneous sea surface, i.e., except for instrumental corrections no other corrections are applied. We refer to these data as the EAPRS-ERS1 dataset. The procedure to derive the along-track DoVs from the observed SSHs for both data sources is briefly outlined in Fig. 3.

4 Results and validation

In this section, we first present and discuss the ability of the extended, vertically referenced DCSM model to represent the time-averaged and instantaneous water levels. Thereafter, we present and validate the NLGEO2013 quasi-geoid and the obtained LAT relative to NLGEO2013 solution.

4.1 The ability of the extended, vertically referenced DCSM model to represent the time-averaged and instantaneous water levels

In Slobbe et al. (2013a), the ability of the model to reproduce both the time-averaged and instantaneous water levels (both computed over the period January 1, 2000–January 1, 2003) was assessed by a comparison with the MDT derived from POL's hindcast, as well as with instantaneous water levels acquired by various radar altimeter satellites (ERS-2, Envisat, GFO-1, Jason-1, and TOPEX/POSEIDON). It was concluded that the model-derived MDT is in good agreement with the MDT derived from POL's hindcast; the SD of

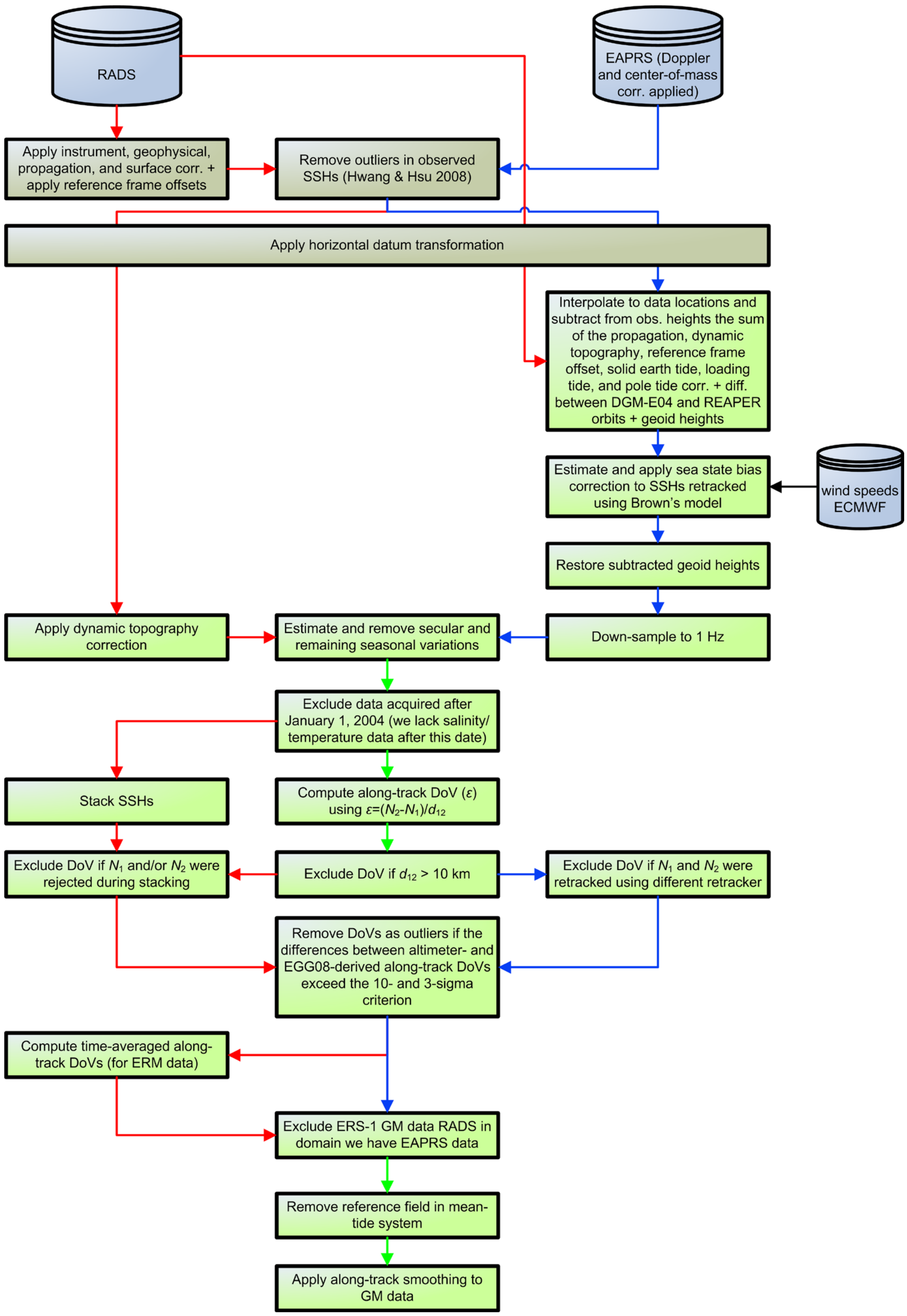

Fig. 3 Flowchart of the procedure used to derive along-track DoV from observed SSHs. The different colors of the blocks refer to the different phases in the overall procedure: (i) *green* refers to a preprocessing step and (ii) *yellow* to a step of the iterative phase (provided iterations are necessary). The different colors of the arrows refer to the different data flows: RADS data (*red*), EAPRS-ERS1 data (*blue*), combined (*green*), and meteorological data (*black*)

the differences is below 2 cm. Larger differences in MDT were observed when comparing the model output with the MDT derived from radar altimeter data and the EGG08 quasi-geoid. Here, we repeat the experiment (i.e., Experiment I of (Slobbe et al. 2013a)) over a much longer time span (January 1, 1984–January 1, 2004). This provides results that are less contaminated by outliers. Figure 4a shows the time-averaged differences between the observed and modeled dynamic topography. The root mean square (RMS) differences are 4.8 cm over the whole model domain and 5.8 cm over the Dutch North Sea. Though the simulation period has been extended by 17 years, overall the differences are very similar to the ones shown in Slobbe et al. (2013a, Fig. 7a). They are attributed to edge effects (along the open sea boundaries), quasi-geoid errors (Celtic Sea), the degraded performance of radar altimetry in coastal regions (English Channel), and errors in the used salinity and temperature fields (northern North Sea).

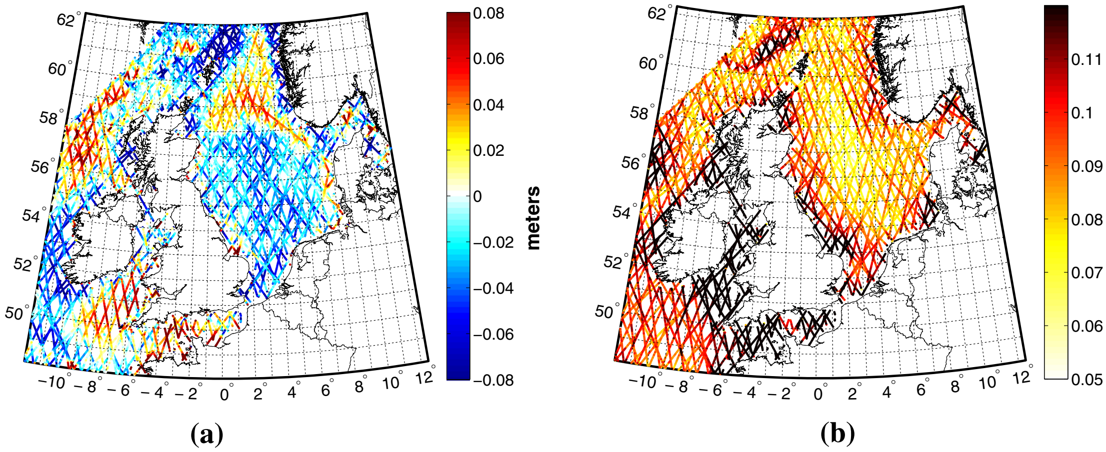

Fig. 4 Time-averaged differences between the observed and modeled dynamic topography at the locations of the radar altimeter data points (**a**), along with the SDs of the differences computed for each bin (**b**)

The RMS differences between observed and modeled instantaneous water levels over the whole model domain vary from 8.2 cm for data acquired by the Envisat satellite to 10.4 cm for data acquired by the GFO-1 satellite. These RMS differences improve to 7.9–10.2 cm over the Dutch North Sea, for data acquired by the TOPEX and GFO-1 satellites, respectively. Figure 4b, however, shows that these latter numbers have little practical implication, since the SD of the differences varies significantly over the model domain; compared to the North Sea, we observe a degraded performance in the Celtic Sea, St. George's Channel, Irish Sea, English Channel, German Bight, and Kattegat. The discrepancies can be partly attributed to the degraded performance of altimetry in coastal regions. Moreover, they can be attributed to (i) the low resolution of the DCSM model and its limited model domain (St. George's Channel and the Irish Sea Holt et al. 2001); (ii) the limited resolution of the wind forcing fields used; (iii) the model's inability to represent the strong tidal currents that exist in the southern North Sea, north of the city Norwich (around (1.5°E, 53.5°N)); and (iv) the model's inability to resolve the large eddies formed by the unstable Norwegian Coastal Current (Huthnance et al. 2009). Furthermore, in Slobbe et al. (2013a), it was shown that about 25 % of these differences can be explained by a bias between the modeled and observed water levels of a single satellite pass. These biases are, among others, attributed to errors in the applied correction for the net steric expansion/contraction of the global oceans. This effect is not captured by DCSM that makes use of the Boussinesq approximation.

4.2 NLGEO2013

NLGEO2013 is computed over the region 15°W–15°E and 46°N–65°N, which is free of edge effects. In practice, it will be used over a much smaller domain, which comprises the Dutch mainland and North Sea (2.5°E–7.2°E and 51.3°N–55.8°N). The reason why we computed it over this large domain is that we want to use it to validate the model-derived LAT solution presented in Sect. 4.3. We use the classical RCR technique, i.e., we reduce all data for the contribution of the global gravity model DGM-1S and estimate the residual signal. The latter is parameterized using spherical radial basis functions (SRBFs) (Klees et al. 2008; Wittwer 2009). Here, we use the Poisson wavelets of order 3, for which an analytical expression is given by Klees et al. (2007, 2008). The parameter vector also contains 64 bias parameters to account for any mutual inconsistencies among the various datasets. The parameters are estimated using least squares. The parameters were estimated using a parallelized linear least squares solver optimized for distributed memory machines (Gunter 2004). Over 80,000 parameters were estimated from approximately 1 Tb of data. Future estimates will make use of an out-of-core solver that can handle problems of arbitrary size (Gunter and van de Geijn 2005), enabling the same approach to be computed over larger areas or with more input measurements.

The SRBFs are located on a Fibonacci grid (González 2010), and individual grid points are omitted if there is no observation available within a distance less than the correlation length of the basis functions. To reduce the computational efforts, the bandwidth (i.e., depth) and the number of the SRBFs are empirically derived over two subregions (cf. Fig. 2): one comprising the Netherlands and the southern North Sea, the other comprising Scotland and the surrounding waters. The combination of bandwidth and number of SRBFs that provides a solution that best fits EGG08 is used in further computations. Based on these experiments, we found a depth of 30 km and a density of one SRBF over ~7.1 km to be optimal; the latter implies 86,569 SRBFs over the computational domain. Exceptions are the UK and Norway. To account for the higher signal variances, a depth of 22.5 km and a density of one SRBF over 4.1 km was chosen empirically.

Contrary to Klees et al. (2008) and Wittwer (2009), the SRBFs are placed on a surface parallel to the topography (land) and bathymetry (ocean). Tenzer et al. (2012) have shown that this approach is superior to the approach of placing them at a constant depth beneath the Bjerhammar sphere. The heights are linearly interpolated from the GEBCO_08 grid (General Bathymetric Chart of the Oceans (GEBCO) 2012); a global 30″ grid generated by combining quality-controlled bathymetric survey data with interpolation between sounding points guided by altimeter-derived bathymetry and, on land, mainly data acquired by the Shuttle Radar Topography Mission.

Monte-Carlo variance component estimation (MCVCE) (Kusche 2003) is applied to obtain proper weight factors for the five observation groups (terrestrial FAAs, airborne gravity disturbances, shipboard FAAs, EGG08-derived DoVs, and altimeter-derived along-track DoVs). For performance reasons, an estimation of the variance components by MCVCE is not feasible for the whole dataset (in future computations we will do so using the aforementioned out-of-core solver). Therefore, we adopt the weights estimated over a subregion that comprises the entire North Sea.

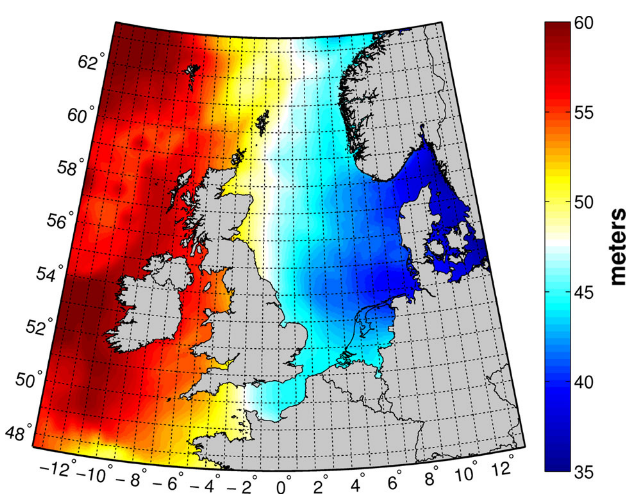

Fig. 5 NLGEO2013 in the ETRS89/GRS80 reference system (zero-tide system). Note that, in the map, we excluded a strip of 1.5° around the boundaries of the computational domain as this is the region that is mostly affected by boundary effects

The NLGEO2013 quasi-geoid is shown in Fig. 5. Table 2 contains the statistics of the differences between NLGEO 2013 and (i) EGG08, and (ii) the gravimetric quasi-geoid solution underlying NLGEO2004 (NLGEO2004-grav) (Crombaghs and de Bruijne 2004). Maps of these differences are shown in Fig. 6.

Based on these maps and the statistics, we observe that NLGEO2013 agrees much better with EGG08 than NLGEO2004-grav. Indeed, this is partially explained by the fact that NLGEO2013 includes DoVs synthesized from EGG08 over the UK and Norway and in areas void of gravity data.

Differences between NLGEO2013 and EGG08 (cf. Fig. 6) are attributed to:

1. The use of different gravity datasets and different pre-processing strategies. This includes the way in which systematic errors in the shipboard gravity data are removed. For example, in this study, we "removed" them by adjusting all shipboard gravity data to the altimeter-derived FAA model DTU10-GRA (Sect. 3.2.1). In the computation of EGG08, a crossover adjustment was applied (Denker and Roland 2005).
2. The use of a different reference field in the RCR procedure. Note that only for NLGEO2013 the reference field includes both GRACE and GOCE data.
3. Differences in the applied RCR technique. In this study, we applied the classical RCR technique. That is, we did not account for uncertainties in the satellite-based geopotential model. In the computation of EGG08, the combination of terrestrial gravity data and the EGM2008 geopotential model up to degree and order 360 (Pavlis et al. 2012) was done by means of spectral weights, which depend on the accuracy of the input datasets (Denker 2013).

Table 2 Statistics of the differences between NLGEO2013 and (i) EGG08, and (ii) NLGEO2004-grav

Model	Area	RMS (cm)	Min (cm)	Max (cm)	Mean (cm)	SD (cm)
EGG08	Oceans + land	2.73	−19.03	28.09	−0.01	2.73
	Oceans	2.73	−19.03	28.09	−0.12	2.73
	Land	2.74	−13.93	19.75	0.16	2.73
	Netherlands	1.42	−4.18	1.08	−1.09	0.91
NLGEO2004-grav[a]	Oceans + land	4.22	−12.8	23.18	0.45	4.19
	Netherlands	2.12	−3.93	3.11	−1.74	1.22

They were computed excluding a strip of 1.5° along the boundaries of the computational domain to exclude edge effects

[a] Differences in vertical datum have been accounted for using values from Ihde and Augath (2002)

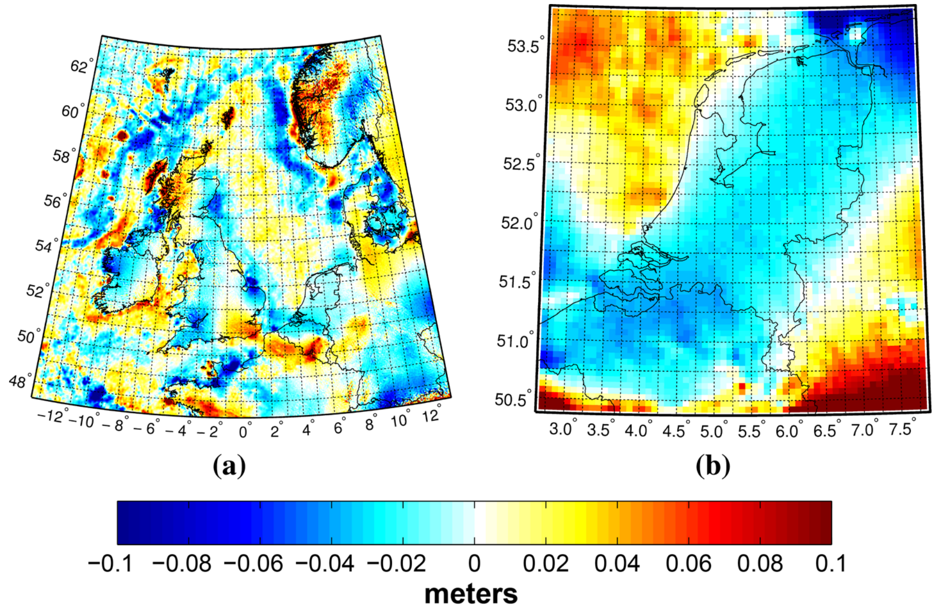

Fig. 6 Differences (without the mean) between NLGEO2013 and EGG08 (**a**) and NLGEO2004-grav (**b**)

4. Differences in the applied data weighting. In this study, MCVCE was used to estimate the variance factors of the different observation groups. In the computation of EGG08, a correlated noise model with an error SD of 1 mGal was used for the terrestrial gravity data in the derivation of the spectral weights (Denker 2013).
5. Differences in the used parameterization. This includes the extension of the functional model by extra bias parameters to account for systematic errors in the gravity datasets. In this study, we used a SRBF parameterization and added 64 bias parameters. In the computation of EGG08, the already mentioned spectral combination technique was used (Denker 2013).
6. The use of different altimeter-derived datasets. This includes the form in which radar altimeter data are used when computing the quasi-geoid and the corrections applied for the sea surface dynamic topography.

A more detailed analysis reveals that the differences along the Norwegian Trench observed in Fig. 6a cannot be solely attributed to the errors in the applied sea surface dynamic topography corrections associated with the errors in POL's salinity and temperature fields (Sect. 4.1). This conclusion is based on a comparison of the observed differences in Fig. 6a and differences between the quasi-geoids obtained with and without including the baroclinic contribution to the applied sea surface dynamic topography corrections (not shown here). The latter are much smaller. Here, it should be noted that due to the errors in POL's salinity and temperature fields, the baroclinic contribution to the DT corrections is overestimated (Slobbe et al. 2013a).

We also validated NLGEO2013 over the Netherlands using geometric height anomalies at 81 GPS/leveling points. The data are provided by the Rijkswaterstaat Data-ICT-Dienst and were also used by Klees et al. (2008). Maps of the differences between the geometric height anomalies, on the one hand, and NLGEO2013, EGG08, and NLGEO2004-grav, on the other hand, are shown in Fig. 7. The statistics of these differences are provided in Table 3. The results indicate that NLGEO2013 has the best performance, with a SD below 1 cm. This is within the uncertainty of the 81 geometric height anomalies (0.010−0.015 m according to Crombaghs and de Bruijne 2004). The two outliers in the south of Limburg are likely caused by local errors in the leveling network (Broekman, personal communication, 2013). When excluding them from the analysis, the SD between the geometric height anomalies and NLGEO2013 reduces to 0.79 cm. The reduction in the differences for NLGEO2013 observed at the points around the IJssel Lake and Wadden Sea, compared to those observed for NLGEO2004-grav, and to a lesser extent EGG08 is explained by the effect of estimating bias parameters for the WADGRAV and Shell shipboard gravity datasets. For these datasets, the estimated bias is −0.45 and −1.18 mGal, respectively. Note that, contrary to what has been done in the computation of NLGEO2004 and NLGEO2007, no corrector surface needs to be added to fit the gravimetric solution to the GPS/leveling points.

4.3 LAT relative to NLGEO2013

To determine the separation between LAT and the NLGEO 2013 quasi-geoid, we run the extended DCSM model over the period 1984–2004. The model is primarily forced by ocean tides. To account for the *average meteorological conditions* in the definition of LAT, the model is also forced by

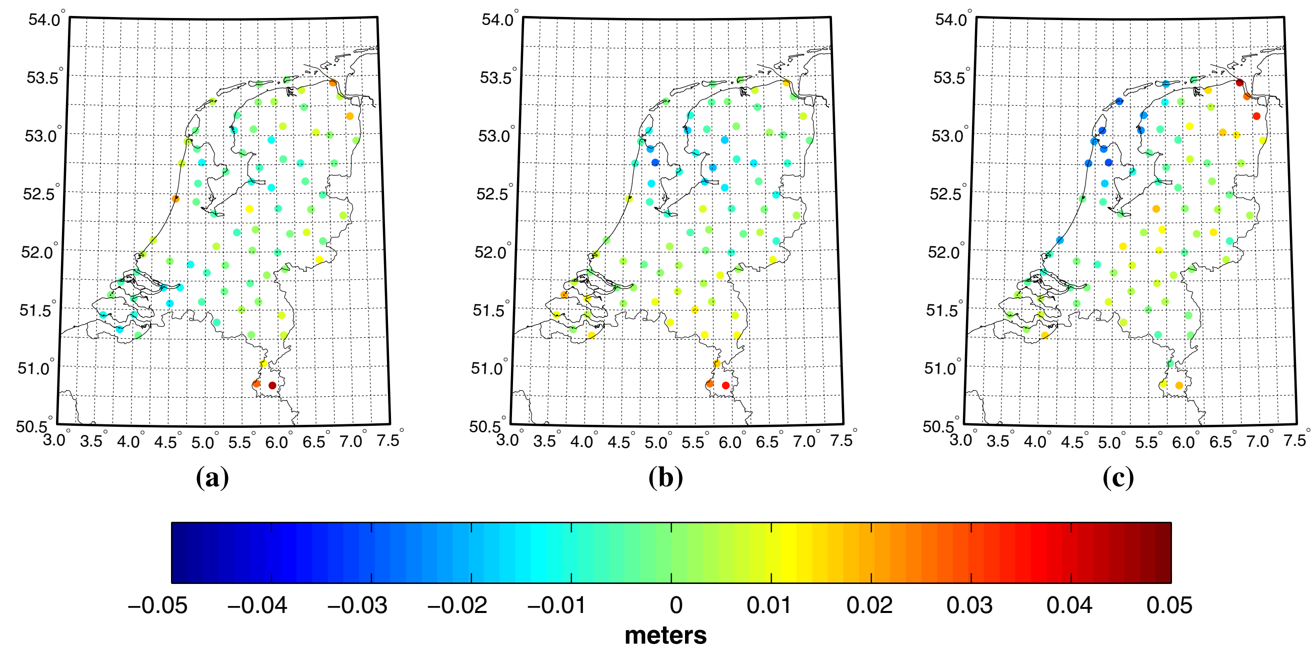

Fig. 7 Residual differences of NLGEO2013 (**a**), EGG08 (**b**), and NLGEO2004-grav (**c**), respectively, at the 81 GPS/leveling points. Note that the mean differences (Table 3) are removed

Table 3 Statistics of the residual differences of NLGEO2013, EGG08, and NLGEO2004-grav, respectively, at the 81 GPS/leveling points

Model	RMS (cm)	Min (cm)	Max (cm)	Mean (cm)	SD (cm)
NLGEO2013	1.34	−0.61	5.43	0.92	0.98
EGG08	2.29	−0.80	5.53	2.03	1.08
NLGEO2004-grav[a]	7.34	−10.20	−3.04	−7.23	1.32

[a] Here, we corrected for the average difference of −68 cm, mentioned by Crombaghs and de Bruijne (2004)

the time-averaged (1984–2004) wind stress fields, mean sea-level pressure fields, and depth-averaged horizontal pressure gradients due to horizontal variations in water density fields. This approach is one of two approaches suggested in Slobbe et al. (2013b). The associated LAT solution (shown in Fig. 8) is adopted by the hydrographic service of the Royal Netherlands Navy. Transition to a LAT solution that includes the dominant time variations (i.e., seasonal) in MSL caused by wind, air pressure, and water density needs to be considered in the future.

Many of the features shown in Fig. 8 are consistent with oceanographic expectations such as coincidence of the locations where the model-derived LAT values approach zero with the well-known amphidromic system in the northwest European continental shelf, and the fact that in the North Sea, the magnitude of the LAT values is largest along the British coast, i.e., where the tidal wave travels southwards. Along the British coast, the shelf is steeper than along the eastern side of the North Sea giving rise to less energy loss due to bottom friction. For more details, we refer to Slobbe et al. (2013b).

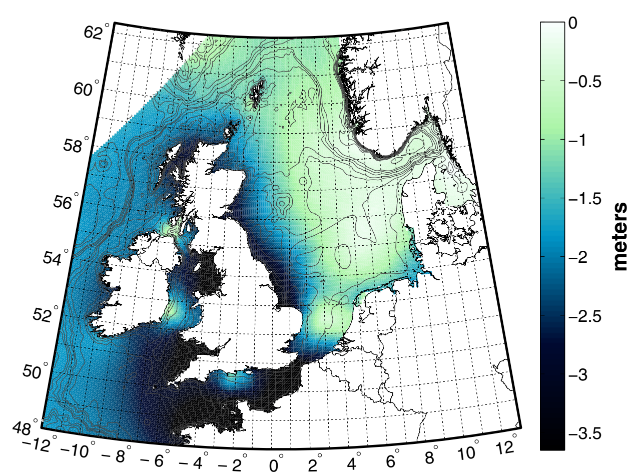

Fig. 8 Lowest astronomical tide relative to NLGEO2013 computed over the entire computation period January 1, 1984—January 1, 2004. The *gray lines* show the *contour lines* of the bathymetry

We validate the model-derived separation between LAT and NLGEO2013 with observation-derived LAT values relative to NLGEO2013 at 92 onshore and 10 offshore tide

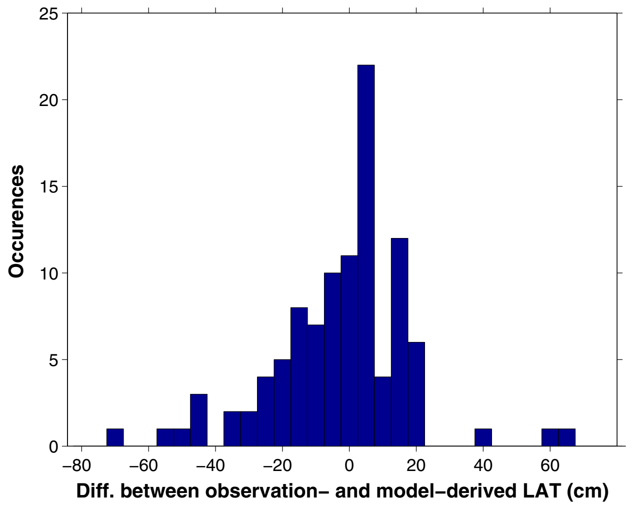

Fig. 9 Histogram of the differences between observation- and model-derived LAT at 102 tide gauges (92 onshore and 10 offshore)

gauges. Figure 9 shows the histogram of the differences at all stations. The differences have a mean of −2.1 cm and a SD of 20.5 cm. Obviously, the differences are larger for the onshore stations. For the 92 onshore tide gauges, we find a mean of −2.2 cm and a SD of 21.5 cm. Whereas for the offshore tide gauges, we obtain a mean of 1.8 cm and a SD of 8.4 cm.

5 Summary and conclusions

We presented an approach to compute consistent realizations of the onshore and offshore VRSs in shallow seas and coastal waters. We have demonstrated the feasibility and performance of this approach for the Dutch mainland and North Sea. The (quasi-)geoid as the onshore VRS plays a central role in this process: it is used to vertically reference water levels of the regional hydrodynamic model; the latter is used to realize the offshore VRS (e.g., LAT as in this study); conversely, the same regional hydrodynamic model is used to correct altimeter-derived sea surface heights or sea surface slopes for the dynamic sea surface topography signal before they are used to compute the (quasi-)geoid. This is what we call a "consistent" realization of onshore and offshore VRSs.

In our approach, LAT is realized by summing the quasi-geoid heights and the model-derived separation between LAT and this quasi-geoid. The latter can be computed from water levels of a vertically referenced regional hydrodynamic model, which comprise the tide and the time-averaged meteorological and baroclinic contributions. Various approaches to realize such a model were identified that differ from each other in the extent and way quasi-geoid information is used. Ideally, the vertical referencing is realized by (i) referring the water levels along the open sea boundaries to the quasi-geoid and (ii) assimilating instantaneous water levels in the model domain into the hydrodynamic model. This strategy requires a proper quasi-geoid model covering the whole domain of the used regional hydrodynamic model. If this is not available, both the quasi-geoid and the vertical referencing of the hydrodynamic model can be realized by an iterative procedure. In this study, however, we follow the approach presented in (Slobbe et al. 2013a) where the vertical referencing is realized by referring the water levels along the open sea boundaries to the quasi-geoid (so, the assimilation of instantaneous water levels is omitted) and the baroclinic component to the prescribed water levels is obtained from an ocean circulation model. For the period January 1, 1984 to January 1, 2004, we found RMS differences between observed and modeled instantaneous and mean dynamic topography of 8–10 and 5.8 cm, respectively, on the Dutch North Sea.

The sea surface dynamic topography corrections obtained from the extended, vertically referenced DCSM model were used to reduce the radar altimeter SSHs to geometric quasi-geoid heights. From these, along-track DoVs were computed that, together with terrestrial, shipboard, and airborne gravity data, and EGG08-derived DoVs in north and east directions, were used to compute the NLGEO2013 quasi-geoid. The quality of NLGEO2013 was assessed by comparing it with both the EGG08 quasi-geoid and the gravimetric quasi-geoid solution underlying NLGEO2004 (NLGEO2004-grav). We conclude that NLGEO2013 best fits to EGG08: the RMS difference over the Netherlands is 1.42 cm. By comparing the NLGEO2013, EGG08, and NLGEO2004-grav quasi-geoids with geometric height anomalies at 81 GPS/leveling points over the Netherlands, it was shown that NLGEO2013 has the best performance. The RMS is below 1.4 cm, which is within the uncertainty of the 81 geometric height anomalies.

Finally, we presented and validated the LAT relative to NLGEO2013 solution. Here, the average meteorological conditions under which the LAT event is supposed to occur, are accounted for by forcing DCSM with ocean tides and the time-averaged (1984–2004) wind stress fields, mean sea-level pressure fields, and depth-averaged horizontal pressure gradients induced by horizontal variations in water density fields. We validate the LAT solution by comparing the observation-derived LAT values relative to NLGEO2013 with the model-derived LAT values. For the 92 onshore tide gauges, we found a mean of −2.2 cm and a SD of 21.5 cm. For the offshore tide gauges, we obtain a mean of 1.85 cm and a SD of 8.4 cm though these numbers are uncertain as we only have 10 offshore tide gauges.

Acknowledgments The authors gratefully acknowledge funding from the Netherlands Vertical Reference Frame (NEVREF) Project. Gravity data were kindly provided by the British Geological Service; the Geological Survey of Northern Ireland; the Nordic Geodetic Commission; Bundesamt für Kartographie und Geodäsie (Germany); Institut für Erdmessung (Germany); the Bureau Gravimétrique International (International Gravity Bureau) IAG service (France); the Banque de données Gravimétriques de la France; and the Bureau de Recherches Géologiques et Minières (France). Tide gauge data were kindly provided by the Vlaamse Hydrografie, Agentschap voor Maritieme Dienstverlening en Kust, afdeling Kust (Belgium); Danish Coastal Authority; Danish Meteorological Institute; Danish Maritime Safety Administration; Service Hydrographique et Océanographique de la Marine (France); Bundesamt für Seeschifffahrt und Hydrographie (Germany); Marine Institute, Ireland; Rijkswaterstaat (the Netherlands); Norwegian Hydrographic Service; Swedish Meteorological and Hydrological Institute; and U.K. National Tidal and Sea Level Facility (NTSLF) hosted by POL. P. A. M Berry is acknowledged for providing retracked ERS-1 radar altimeter data and O.B. Andersen for providing the mean sea surface heights and altimeter-derived gravity anomaly grids to the community. In addition, the authors gratefully acknowledge the support of the Proudman Oceanographic Laboratory (POL) for providing the results of the Atlantic—European North West Shelf—Ocean Physics Hindcast to the community and their help in answering some questions. We also acknowledge the valuable comments of three anonymous reviewers.

References

Andersen OB (2010) The DTU10 global gravity field and mean sea surface—improvements in the Arctic. http://www.space.dtu.dk/english/Research/Scientific_data_and_models/Global_Marine_Gravity_Field, Second international symposium of the gravity field of the Earth (IGFS2), Fairbanks, Alaska

Andersen OB, Knudsen P (2000) The role of satellite altimetry in gravity field modelling in coastal areas. Phys Chem Earth 25(1):17–24. doi:10.1016/S1464-1895(00)00004-1

Andersen OB, Knudsen P, Berry P (2010) The DNSC08GRA global marine gravity field from double retracked satellite altimetry. J Geod 84(3):191–199. doi:10.1007/s00190-009-0355-9

Carrère L, Lyard F (2003) Modeling the barotropic response of the global ocean to atmospheric wind and pressure forcing—comparisons with observations. Geophys Res Lett 30(6):n/a-n/a, doi:10.1029/2002GL016473

Crombaghs M, de Bruijne A (2004) NLGEO2004—een nieuw geoïdemodel voor Nederland. Technical report, Adviesdienst Geo-informatie en ICT, Report AGI-GAP-2004-25, Delft, 41 p

Dee DP, Uppala SM, Simmons AJ, Berrisford P, Poli P, Kobayashi S, Andrae U, Balmaseda MA, Balsamo G, Bauer P, Bechtold P, Beljaars ACM, van de Berg L, Bidlot J, Bormann N, Delsol C, Dragani R, Fuentes M, Geer AJ, Haimberger L, Healy SB, Hersbach H, Hólm EV, Isaksen L, Kållberg P, Köhler M, Matricardi M, McNally AP, Monge-Sanz BM, Morcrette JJ, Park BK, Peubey C, de Rosnay P, Tavolato C, Thépaut JN, Vitart F (2011) The ERA-Interim reanalysis: configuration and performance of the data assimilation system. QJ R Meteor Soc 137(656):553–597. doi:10.1002/qj.828

Deng X (2003) Improvement of Geodetic Parameter Estimation in Coastal Regions from Satellite Radar Altimetry. Phd, Curtin University of Technology, Department of Spatial Sciences

Deng X, Featherstone WE, Hwang C, Berry PAM (2002) Estimation of contamination of ERS-2 and POSEIDON satellite radar altimetry close to the coasts of Australia. Mar Geod 25(4):249–271

Denker H (2013) Regional gravity field modeling: theory and practical results. In: Xu G (ed) Sciences of Geodesy—II, Springer, Berlin, Heidelberg, pp 185–291. doi:10.1007/978-3-642-28000-9_5

Denker H, Roland M (2005) Compilation and evaluation of a consistent marine gravity data set surrounding europe. In: A window on the future of geodesy. Springer, Berlin, Heidelberg, pp 248–253. doi:10.1007/3-540-27432-4_42

Farahani HH, Ditmar P, Klees R, Liu X, Zhao Q, Guo J (2013a) The static gravity field model DGM-1S from GRACE and GOCE data: computation, validation and an analysis of GOCE mission's added value. J Geod 87(9):843–867. doi:10.1007/s00190-013-0650-3

Farahani HH, Ditmar P, Klees R, Liu X, Zhao Q, Guo J (2013b) Validation of static gravity field models using GRACE K-band ranging and GOCE gradiometry data. Geophys J Int 194:751–771. doi:10.1093/gji/ggt149

Forsberg R, Hehl K, Mayer U, Gidskehaug A, Bastos L (1997) Development of an airborne geoid mapping system for coastal oceanography (AGMASCO). In: Proceedings of international symposium on gravity geoid and marine geodesy, Japan, pp 130–142

General Bathymetric Chart of the Oceans (GEBCO) (2012) General bathymetric chart of the oceans (GEBCO). http://www.gebco.net/. Accessed Mar 7, 2013

Gerritsen H, de Vries H, Philippart M (1995) The Dutch continental shelf model. In: Lynch DR, Davies AM (eds) Quantitative skill assessment for coastal ocean models, Coastal Estuarine Stud., vol 47, AGU, Washington, DC, pp 425–467. doi:10.1029/CE047p0425

Gommenginger C, Thibaut P, Fenoglio-Marc L, Quartly G, Deng X, Gómez-Enri PJ, Challenor YG (2011) Retracking altimeter waveforms near the coasts. In: Vignudelli S, Kostianoy AG, Cipollini P, Benveniste J (eds) Coastal altimetry, 1st edn. Springer, Berlin, Heidelberg, pp 61–101

González Á (2010) Measurement of areas on a sphere using Fibonacci and latitude–longitude lattices. Math Geosci 42(1):49–64. doi:10.1007/s11004-009-9257-x

Gunter BC (2004) Computational methods and processing strategies for estimating earth's gravity field. PhD thesis, The University of Texas at Austin. http://repositories.lib.utexas.edu/handle/2152/1318

Gunter BC, van de Geijn RA (2005) Parallel out-of-core computation and updating of the QR factorization. ACM Trans Math Softw 31(1):60–78. doi:10.1145/1055531.1055534

Haagmans RHN, Husti GJ, Plugers P, Smit JHM, Strang van Hees GL (1988) NAVGRAV Navigation and Gravimetric Experiment at the North Sea. Technical report 32, Netherlands Geodetic Commission, Delft

Holt JT, James ID (2001) An s coordinate density evolving model of the northwest European continental shelf, 1. Model description and density structure. J Geophys Res 106:14015–14034. doi:10.1029/2000JC000304

Holt JT, James ID, Jones JE (2001) An s coordinate density evolving model of the northwest European continental shelf, 2. Seasonal currents and tides. J Geophys Res 106:14035–14054. doi:10.1029/2000JC000303

Holt JT, Allen JI, Proctor R, Gilbert F (2005) Error quantification of a high-resolution coupled hydrodynamic ecosystem coastal ocean model: part 1 model overview and assessment of the hydrodynamics. J Mar Syst 57(1–2):167–188. doi:10.1016/j.jmarsys.2005.04.008

Horsburgh KJ, Wilson C (2007) Tide-surge interaction and its role in the distribution of surge residuals in the North Sea. J Geophys Res 112(C8):n/a–n/a. doi:10.1029/2006JC004033

Hughes CW, Bingham RJ (2008) An oceanographer's guide to GOCE and the geoid. Ocean Sci 4:15–29

Huthnance JM, Holt JT, Wakelin SL (2009) Deep ocean exchange with west-European shelf seas. Ocean Sci 6:1061–1092

Hwang C, Hsu HY (2008) Shallow-water gravity anomalies from satellite altimetry: case studies in the east china sea and Taiwan strait. J Chin Inst Eng 31(5):841–851. doi:10.1080/02533839.2008.9671437

Hwang C, Guo J, Deng X, Hsu HY, Liu Y (2006) Coastal gravity anomalies from retracked geosat/GM altimetry: improvement, limitation and the role of airborne gravity data. J Geod 80:204–216. doi:10.1007/s00190-006-0052-x

Ihde J, Augath W (2002) The European vertical reference system (EVRS), its relation to a world height system and to the ITRS. Vistas for geodesy in the new millennium, pp 78–83

Iliffe JC, Ziebart MK, Turner JF (2007) A new methodology for incorporating tide gauge data in sea surface topography models. Mar Geod 30(4):271–296. doi:10.1080/01490410701568384

International Hydrographic Organization (1994) Hydrographic dictionary part I, vol I, English. http://www.iho.int/iho_pubs/standard/S-32/S-32-eng.pdf, special publication no. 32, 5th edn

International Hydrographic Organization (2011) Resolutions of the International Hydrographic Organization. www.iho.int, publication M-3, 2nd edn, 2010, updated to August 2011

Klees R, Prutkin I, Tenzer R, Wittwer T (2007) Development of a technique for combining parameters of the Earth's gravity field for quasi-geoid determination on the territory of the Federal Republic of Germany and Europe. Technical report, Delft University of Technology

Klees R, Tenzer R, Prutkin I, Wittwer T (2008) A data-driven approach to local gravity field modelling using spherical radial basis functions. J Geod 82:457–471. doi:10.1007/s00190-007-0196-3

Kusche J (2003) A Monte-Carlo technique for weight estimation in satellite geodesy. J Geod 76:641–652. doi:10.1007/s00190-002-0302-5

Leendertse JJ (1967) Aspects of a computational model for long-period water-wave propagation. Rand Corporation for the United States Air Force Project Rand, California

Myers EP, Wong A, Hess KW, White SA, Spargo E, Feyen J, Yang Z, Richardson P, Auer C, Sellars J, Woolard J, Roman D, Gill S, Zervas C, Tronvig K (2005) Development of a national VDatum, and its application to sea level rise in North Carolina. Downloaded from http://www.thsoa.org/hy05/09_3.pdf, technical paper presented at the U.S. Hydro 2005 conference

Parker B, Milbert D, Hess K, Gill S (2003) National vdatum—the implementation of a national vertical datum transformation database. U.S. Hydrographic conference 2003 proceedings/technical papers

Pavlis NK, Holmes SA, Kenyon SC, Factor JK (2012) The development and evaluation of the earth gravitational model 2008 (egm2008). J Geophys Res 117(B4):n/a–n/a. doi:10.1029/2011JB008916

Pineau-Guillou L, Dorst LL (2011) Creation of vertical reference surfaces at sea using altimetry and GPS. Ann Hydrograph 8(777):10-1–10-7. http://www.shom.fr/fr_prod_annales/777/777-ZTL.pdf

Prandle D (1978) Residual flows and elevations in the Southern North Sea. Proc R Soc Lond A 359:189–228. doi:10.1098/rspa.1978.0039

Prandle D, Wolf J (1978) The interaction of surge and tide in the North Sea and River Thames. Geophys J Int 55:203–216. doi:10.1111/j.1365-246X.1978.tb04758.x

Ray RD (1999) A global ocean tide model from TOPEX/POSEIDON altimetry: GOT99.2. Technical report, Goddard Space Flight Center, Greenbelt, NASA Tech. Memo 209478, 58 pp

Sandwell DT, Smith WHF (2009) Global marine gravity from retracked Geosat and ERS-1 altimetry: ridge segmentation versus spreading rate. J Geophys Res 114(B1):n/a–n/a. doi:10.1029/2008JB006008.

Schäfer U, Liebsch G, Schirmer U, Ihde J, Olesen AV, Skourup H, Forsberg R, Pflug H, Neumeyer J (2008) Improving gravity field modelling in the German-Danish border region by combining airborne, satellite and terrestrial gravity data. In: IAG International symposium on gravity, geoid and earth observation (Chania, Greece 2008)

Scharroo R (2013) RADS version 3.1: user manual and format specification. Delft University of technology (Accessed June 2013). http://rads.tudelft.nl/rads/radsmanual.pdf

Slobbe DC, Klees R (2014) The impact of the dynamic sea surface topography on the quasi-geoid in shallow coastal waters. J Geod 88:241–261. doi:10.1007/s00190-013-0679-3

Slobbe DC, Verlaan M, Klees R, Gerritsen H (2013a) Obtaining instantaneous water levels relative to a geoid with a 2D storm surge model. Cont Shelf Res 52:172–189. doi:10.1016/j.csr.2012.10.002

Slobbe DC, Klees R, Verlaan M, Dorst LL, Gerritsen H (2013b) Lowest astronomical tide in the North Sea derived from a vertically referenced shallow water model, and an assessment of its suggested sense of safety. Mar Geod 36(1):31–71. doi:10.1080/01490419.2012.743493

Stelling GS (1984) On the construction of computational methods for shallow water flow problems. PhD thesis, Delft University of Technology, Delft, Rijkswaterstaat communications 35

Tenzer R, Prutkin I, Klees R (2012) A comparison of different integral-equation-based approaches for local gravity field modelling: case study for the Canadian rocky mountains. In: Kenyon S, Pacino MC, Marti U (eds) Geodesy for planet Earth, international association of geodesy symposia, vol 136, Springer, Berlin Heidelberg, pp 381–388. doi:10.1007/978-3-642-20338-1_46

Turner JF, Iliffe JC, Ziebart MK, Wilson C, Horsburgh KJ (2010) Interpolation of tidal levels in the coastal zone for the creation of a hydrographic datum. J Atmos Ocean Tech 27:605–613. doi:10.1175/2009JTECHO645.1

Verlaan M, Zijderveld A, de Vries H, Kroos J (2005) Operational storm surge forecasting in the Netherlands: developments in the last decade. Philos Trans R Soc Math Phys Eng Sci 363:1441–1453. doi:10.1098/rsta.2005.1578

Wittwer TF (2009) Regional gravity field modelling with radial basis functions. PhD thesis, Delft University of Technology, Nederlandse Commissie voor Geodesie Publikatie 72

Wolf J (1981) Surge-tide interaction in the North Sea and River Thames. In: Peregrine DH (ed) Floods due to high winds and tides. Elsevier, New York, pp 75–94

Ziebart MK, Iliffe JC, Turner JF, Oliveira J, Adams R (2007) VORF—The UK vertical offshore reference frame: enabling real-time hydrographic surveying. In: Proceedings of ION GNSS2007, Fort Worth, Texas, USA